An efficient strategy for the acquisition of weak galileo E1 OS signals

Myriam Foucras, Olivier Julien, Christophe Macabiau, Bertrand Ekambi

An Efficient Strategy for the Acquisition of Weak Galileo E1 OS Signals

Myriam Foucras [1, 2], Olivier Julien [2], Christophe Macabiau [2], and Bertrand Ekambi [1]
[1] ABBIA GNSS Technologies, Toulouse, France
mail: {myriam.foucras ; bertrand.ekambi}@abbia.fr
[2] ENAC, Toulouse, France
mail: {foucras; ojulien; macabiau}@recherche.enac.fr

***Abstract* – Acquisition is the first process of a GNSS receiver and is also the process which needs the most resources. Moreover, acquiring of weak Galileo E1 OS signals is a real challenge due to the presence of frequent (potentially at each spreading code period) bit transitions (data bit on the data component and secondary code chip on the pilot component). After a study of the effects of data modulation, two acquisition strategies, one bit transition insensitive and the other not, are developed and brought face to face on performance criteria such as: execution time, probability of detection, probability of false alarm…**

BIOGRAPHIES

Myriam FOUCRAS received her Masters in Mathematical engineering and Fundamental Mathematics from the University of Toulouse in 2009 and 2010. Since 2011, she is a PhD. student at the Signal Processing and Navigation (SIGNAV) research group of the TELECOM laboratory of Ecole Nationale de l'Aviation Civile (ENAC). Funded by ABBIA GNSS Technologies, in Toulouse, France, her work consists in the development of a GPS/Galileo software receiver.

Olivier JULIEN is the head of the Signal Processing and Navigation (SIGNAV) research group of the TELECOM laboratory of ENAC, in Toulouse, France. His research interests are GNSS receiver design, GNSS multipath and interference mitigation and GNSS interoperability. He received his engineer degree in 2001 in digital communications from ENAC and his PhD in 2005 from the Department of Geomatics Engineering of the University of Calgary, Canada.

Christophe MACABIAU graduated as an electronics engineer in 1992 from the ENAC in Toulouse, France. Since 1994, he has been working on the application of satellite navigation techniques to civil aviation. He received his PhD. in 1997 and has been in charge of the TELECOM laboratory of the ENAC since 2011.

Bertrand EKAMBI graduated by a Master in Mathematical Engineering in 1999. Since 2000, he is involved in the main European GNSS projects: EGNOS and GALILEO. He is the founder manager of ABBIA GNSS Technologies, a French SME working on Space Industry, based in Toulouse, France.

I. INTRODUCTION

The overall context of this work is the development of a GPS/Galileo single frequency (L1) software receiver. This GNSS receiver is meant for educational and research purposes. These kinds of applications need a high level of flexibility and reconfigurability, which can be provided by the software receiver technology.

The first stage of the GNSS signal processing is the acquisition process, which gives a rough estimation of the code delay and Doppler frequency of the incoming signal. The objective of the developed GNSS software receiver is, in cold start mode, to provide the first position in 60 seconds for a received GPS or Galileo signal of 27 dBHz with a high probability (90% of time for any given incoming Doppler frequency and code delay). These values were fixed after a specification review of currently sold receivers – hardware and software (Receiver surveys in [1]–[3]). The probability of false alarm of the acquisition process is set to 10^{-7} corresponding to around one false alarm.

One clearly understands that the main challenges of the acquisition process are:

- Trying a high number of code delay/Doppler frequency couples in a short period of time
- Enabling the acquisition of weak signals with a high probability

Both challenges are antagonist because the acquisition of weak signals is very complex and needs a lot of operations, leading to a longer acquisition execution time. So a compromise between these two objectives should be found.

The efficient and fast acquisition of Galileo E1 OS signal is still a challenge compared to GPS L1 C/A signal due to its features, discussed in section II. The need for a specific acquisition strategy for Galileo E1 OS is thus clearly justified and is the aim of this paper. To try to answer this, two acquisition strategies are presented, studied and brought face to face. Because the effects of a bit transition are not negligible as discussed later, the first one deals with a bit transition insensitive acquisition method -the DBZPTI- which was developed by the authors and presented in [4]. The second one can be seen as the classical acquisition method of a signal made of two components.

Moreover, both acquisition strategies are developed in view of an implementation on a software GNSS receiver developed in C++.

The outline of the paper is as follows:

- The first part serves to review the Galileo E1 OS signal and presents the considered reception platform.
- The second part describes the classical Galileo E1 OS acquisition method, this acquisition method is the base of one acquisition strategy and of the verification step.
- The third part covers in detail the impact of a bit transition on the acquisition performance in order to highlight the interest of a bit transition insensitive acquisition method.
- The fourth part focuses on the DBZPTI, the transition insensitive acquisition method which is the base of the proposed efficient acquisition strategy.
- The fifth part is dedicated to the comparison of the acquisition strategies by studying the choice of the parameters and the performance. A comparison of the execution time (based on Matlab simulations) is given at the end of this part to demonstrate the computational efficiency of the proposed acquisition strategy.
- The last part concludes the paper, remaining the main points of interests and results.

The innovative contributions of this paper consist in:

- Studying the effects of a bit transition on the Galileo E1 OS signal acquisition performance
- Improving the DBZPTI leading to degradation performance comparable to classical acquisition method (around 1 dB in the worst case instead of 8 dB)
- Developing an efficient strategy for the acquisition of weak Galileo E1 OS signals

II. Galileo E1 OS Signal Model and Considered Reception Platform

A. Galileo E1 OS signal characteristics

The Galileo E1 OS is located in the L1 band and its center frequency is 1575.42 MHz. Its main features are [5]:

- PRN sequences are 4092-chip long and transmitted at a rate of 1.023 Mchip/s
- The Galileo E1 OS data bit rate is 250 bit/s meaning a data bit duration of 4 ms
- Presence of two components: a data component containing the navigation message and a dataless pilot component, which is characterized by a known secondary code that modulates the primary spreading code. Both components are synchronized and carry 50% of the total signal power
- The Galileo E1 OS spreading codes' period have the same duration as a data or secondary code bit (4 ms). This implies that a transition (data bit and/or secondary code chip) occurs at each spreading code period with a probability close to 50%.
- The modulation of the Galileo E1 OS signal is CBOC(6,1,1/11)

The expression of the received Galileo E1 OS signal (for one satellite) is given by (1) [5].

$$r(t) = A\begin{bmatrix} d(t-\tau)c_{1,D}(t-\tau)p_{CBOC,D}(t-\tau) \\ -c_2(t-\tau)c_{1,P}(t-\tau)p_{CBOC,P}(t-\tau) \end{bmatrix} \times cos(2\pi f_{IF}t + \phi) + n(t) \quad (1)$$

Where

- r is the received signal at time t
- $A = \sqrt{P}$ is the amplitude of the incoming signal at the correlator output on each component
- τ is the delay of the spreading code
- d is the data sequence
- $c_{1,D}$ and $c_{1,P}$ are the spreading codes carried by the data and pilot components
- c_2 is the known secondary code
- f_{IF} is the intermediate frequency
- ϕ is the phase of the signal including Doppler frequency of the incoming signal f_D
- n is the noise (assumed white Gaussian)
- $p_{CBOC,D}$ and $p_{CBOC,P}$ are the sub-carriers carried by the data and pilot components

$$p_{CBOC,D}(t) = \frac{\sqrt{10}\, sign(\sin(2\pi f_{sc}t)) + sign(\sin(2\pi 6 f_{sc}t))}{\sqrt{11}}$$
$$p_{CBOC,P}(t) = \frac{\sqrt{10}\, sign(\sin(2\pi f_{sc}t)) - sign(\sin(2\pi 6 f_{sc}t))}{\sqrt{11}} \quad (2)$$

Where $f_{sc} = 1.023\ MHz$ is the sub-carrier frequency

The first part in (1) $d(t)c_{1,D}(t-\tau)p_{CBOC,D}(t-\tau)$ represents the data component with the navigation message and the spreading code. The second term $c_2(t)c_{1,P}(t-\tau)p_{CBOC,P}(t-\tau)$ represents the pilot component with the secondary code and a different spreading code.

B. Considered Reception Platform

The hardware equipment of the GNSS software receiver is composed of:

- A laptop (Intel Core i7, 4 GiB RAM, 8 cores)
- An IFEN RF front-end [6] with:
  - Sampling frequency: $f_s = 20.48$ MHz
  - Intermediate frequency: $f_{IF} = 5.5$ MHz
  - RF bandwidth: $B = 15$ MHz

Let us note that a BOC(1,1) is locally generated (instead of a CBOC(6,1,1/11)) and $R_{c_{1,D}/c_{1,P}}$ the cross-correlation between $c_{1,D}$ and $c_{1,P}$ is considered negligible due to the almost orthogonality of codes.

In this paper, the integration time T_I is fixed at $T_I = 4$ ms (spreading code period), this leads to a sampled signal of length 81920.

III. Classical Galileo E1 OS Acquisition Scheme

A. Initial Acquisition based on Non-Coherent Combining

There are several techniques that have been proposed for the acquisition of the Galileo E1 OS signal. So the main acquisition methods are reviewed to lead to the choice of two acquisition methods which will be studied more in detail in this paper.

Since the context of the work is an optimized acquisition adapted to the reception of weak Galileo E1 OS signal, acquisition methods based on the the pilot component alone is incongruous because only half of the useful power is considered ([7], [8]). Thus, to acquire weak Galileo E1 OS signal, the totality of the useful signal power needs to be employed. There are several acquisition methods which combine both components.

The non-coherent combining acquisition method was largely studied for Galileo E1 OS ([9], [10]) or for GPS L5 signals and Galileo E5a, E5b signals [8]. The received signal is correlated separately with the local spreading codes of the data and pilot component. The four (two in-phase and quadrature) correlation outputs are then squared and summed together. The scheme of the method is presented in Figure 1.

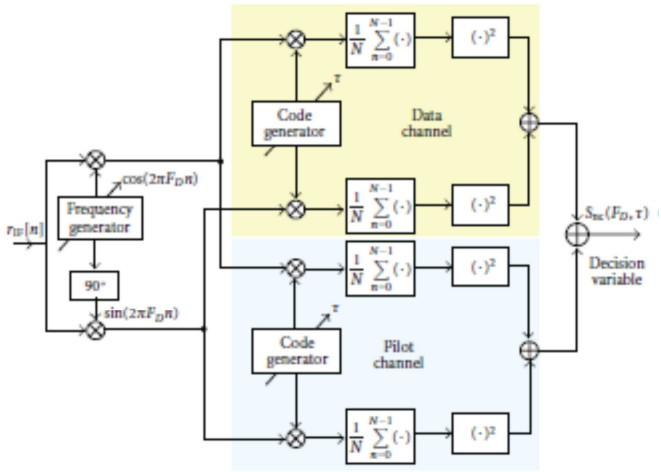

Figure 1: Non-coherent combining acquisition method [9]

This method is retained as the reference method and called the "classical acquisition method" throughout this paper because it is widely referenced. The mathematical model and statistic performance of this acquisition method is given in Appendix A.

In a context of an optimized acquisition strategy, correlations are computed using fast Fourier transforms (FFT), leading to a negligible uncertainty on the code delay (half of the sampling period). The uncertainty on the Doppler frequency error (due to Doppler bins of size $1/(2T_I)$) leads to a worst case degradation of 0.9 dB.

However, this method is not insensitive to bit transitions and one of the aim of this paper is to explain the associated degradation (section IV).

B. Verification step using M of N Technique

After the initial detection, a verification step always needs to be implemented. This step consists in eliminating the false alarms and verifying the detection of the "right bin" (right Doppler frequency and right code delay).

Two main acquisition techniques are generally proposed: the Tong detector [11] and the M of N technique [11], [12]. They take independent correlation outputs computed with the same parameters (Doppler frequency and code delay) and compare them to a threshold (determined according to a desired probability of false alarm). For the M of N technique, if at least M of the N detectors exceed the threshold, the signal is declared present, the signal is declared absent otherwise, so it can be modeled as a binomial distribution. Figure 2 completes the description.

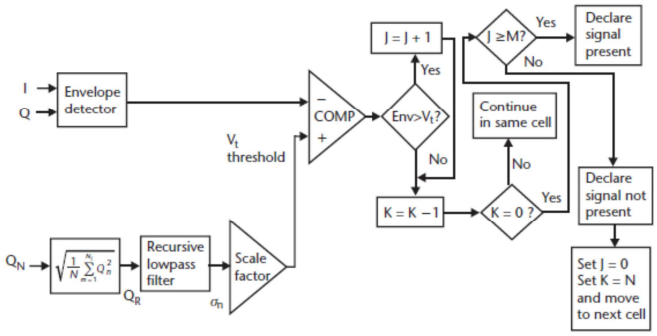

Figure 2: M of N scheme [13]

The M of N technique consists in verifying the detection of the right bin, so to not fail, the immediate surrounding bins are also verified. Moreover, the context (acquisition of weak signals) leads to do non-coherent integrations for each detector.

This concludes the second part where the classical acquisition method was presented.

IV. The Effect of Data Transition on the Initial Acquisition Step

A. Expression of the correlator outputs in presence of bit transition

To study the effect of data modulation, let us first examine its effect on classical correlator outputs. The data and secondary code bit transitions can occur at each spreading code period with a probability of roughly ½ (for the secondary code of 25 chips, there are 12 chip transitions). Thus, it is essential to understand the effects of a bit transition taking place at $t_0 \in [kT_I; (k+1)T_I]$.

Without loss of generalities, the values of the data bit $d(t)$ in (3) are assumed to be such that:

$$d(t) = \begin{cases} 1, kT_I \le t < t_0 \\ -1, t_0 \le t \le (k+1)T_I \end{cases}$$

The acquisition detector $T_{t_0}(k, \varepsilon_{f_d})$ can be computed after the evaluation of the in-phase and quadrature correlator outputs I_{t_0} and Q_{t_0} which depend on the instant of bit transition t_0 (the development is in Appendix D).

$$\begin{aligned} T_{t_0}(k, \varepsilon_{f_D}) &= I_{t_0}^2(k, \varepsilon_{f_D}) + Q_{t_0}^2(k, \varepsilon_{f_D}) \\ &= \frac{A^2}{4} R^2(\varepsilon_\tau(k)) \frac{1}{(\pi \varepsilon_{f_D} T_I)^2} \times \\ &\begin{pmatrix} 1 + \cos^2(\pi \varepsilon_{f_D} T_I) \\ -2\cos(\pi \varepsilon_{f_D} T_I) \cos\left(\pi \varepsilon_{f_D} (T_I(2k+1) - 2t_0)\right) \end{pmatrix} \end{aligned} \quad (3)$$

Where

- ε_{f_D} is the Doppler frequency error
- R stands for $R_{c_1,D}$ or $R_{c_1,P}$

As observed in [14] (for the GPS L1 C/A signal) and visible on Figure 3, the power attenuation at the correlator output due to a bit transition is not independent from the Doppler frequency error.

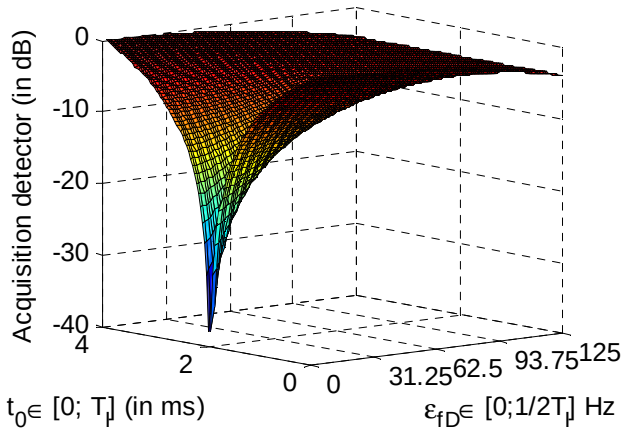

Figure 3: Effects of a bit transition on the acquisition detector

The worst location of a bit transition is at $t_0 = kT_I + \frac{T_I}{2}$ which corresponds to the center of the integration interval. In this case, the detector value is:

$$\begin{aligned} T_{kT_I + \frac{T_I}{2}}(k, \varepsilon_{f_D}) &= I^2_{kT_I + \frac{T_I}{2}}(k, \varepsilon_{f_D}) + Q^2_{kT_I + \frac{T_I}{2}}(k, \varepsilon_{f_D}) \\ &= \frac{A^2}{4} R^2(\varepsilon_\tau(k)) \times \left(\frac{1 - \cos(\pi \varepsilon_{f_D} T_I)}{\pi \varepsilon_{f_D} T_I} \right)^2 \end{aligned} \quad (4)$$

And $T_{kT_I + \frac{T_I}{2}}(k, \varepsilon_{f_D}) = 0$ if $\varepsilon_{f_D} = 0$. This confirms that the power of the detector is null when a data bit transition occurs exactly in the middle of the integration period for the right Doppler bin as already shown in [4].

The worst case, in the frequency domain and for any location of the bit transition, is for $\varepsilon_{f_D} = \frac{1}{2T_I}$, which corresponds to the maximal Doppler frequency error. In this case, $\cos(\pi \varepsilon_{f_D} T_I) = 0$ and so, the detector is equal to (5) and the associated losses are around 4 dB.

$$T_{t_0}\left(k, \frac{1}{2T_I}\right) = \frac{A^2}{4} R^2(\varepsilon_\tau(k)) \times \frac{4}{\pi^2} \quad (5)$$

As it can be seen with (5), the instant of the bit transition has absolutely no effect on the detector when the Doppler error is of $\frac{1}{2T_I}$.

B. Performance Degradation due to bit transition

Now, let us study the effects of data modulation on longer non-coherent integrations of the totality of the Galileo E1 OS signal (data and pilot components). Let us assume that K non-coherent integrations on $T_I = 4$ ms are performed and let us evaluate the resulting probability of detection based on a hypothesis test (Appendix A).

Expressing the probability of detection shows that the bit transition location influences the non-centrality parameter λ_u of the distribution of the acquisition detector. The presence of a bit transition is marked by the variable u.

$$\begin{cases} no\ bit\ transition & u = 0 \quad \lambda_u(k) = \lambda_0(k) \\ bit\ transition\ at\ t_0 & u = 1 \quad \lambda_u(k) = \lambda_{t_0}(k) \end{cases} \quad (6)$$

Where

$$\lambda_0 = \frac{A^2}{4} R^2(\varepsilon_\tau(k)) \mathrm{sinc}^2(\pi \varepsilon_{f_D} T_I) \quad (7)$$

$$\begin{aligned} \lambda_{t_0} &= \frac{A^2}{4} R^2(\varepsilon_\tau(k)) \times \frac{1}{(\pi \varepsilon_{f_D} T_I)^2} \times \\ &\begin{pmatrix} 1 + \cos^2(\pi \varepsilon_{f_D} T_I) \\ -2\cos(\pi \varepsilon_{f_D} T_I) \cos\left(\pi \varepsilon_{f_D} (T_I(2k+1) - 2t_0)\right) \end{pmatrix} \end{aligned} \quad (8)$$

Knowing that the bit transition occurs with an average probability of $\frac{1}{2}$ and that data bit transition is independent from secondary code chip transition but synchronized, the probability of detection can be determined. Assuming, as an example, that $K = 1$ (one coherent integration), there can be l bit transitions (with l equals to 0, 1 or 2). For each case, the probability of occurrence P_l and the probability of detection with l bit transitions P_{d_l} are evaluated.

- $l = 0$ (0 bit transition):

The probability that there is no bit transition is $P_0 = \frac{1}{2} \times \frac{1}{2}$ and in this case the probability of detection is $P_{d_0} = F^{-1}_{\chi^2(4K)}(2\lambda_0)$

- $l = 1$: data or secondary code bit transition

The probability of 1 bit transition is $P_1 = \binom{2}{1} \times \frac{1}{2} \times \frac{1}{2}$ and the probability of detection is:

$$P_{d_1} = F^{-1}_{\chi^2(4K)}(\lambda_0 + \lambda_{t_0})$$

- $l = 2$: data and secondary code bit transitions

The probability of 2 bit transitions is $P_2 = \frac{1}{2} \times \frac{1}{2}$ and the probability of detection is $P_{d_2} = F^{-1}_{\chi^2(4K)}(2\lambda_{t_0})$.

At the end, the average probability of detection for $K = 1$ is:

$$P_{d,t_0} = \sum_{l=0}^{2} P_l \times P_{d_l} = \frac{1}{4}P_{d_0} + \frac{1}{2}P_{d_1} + \frac{1}{4}P_{d_2} \qquad (9)$$

The representation of the 3 probabilities of detection P_{d_0}, P_{d_1} and P_{d_2} versus C/N_0 is given by the Figure 4 (worst case for t_0 in the midlle of the integration interval and for $\varepsilon_{f_D} = 0$ Hz and $K = 1$).

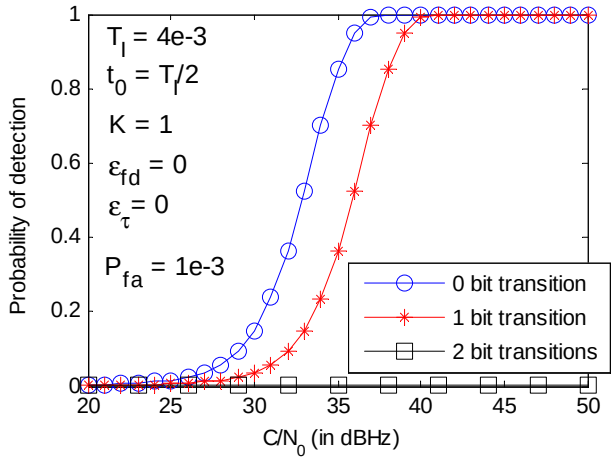

Figure 4: Probabilities of detection for 0, 1 or 2 bit transitions

In conclusion, the probability of detection P_{d,t_0} for any K is:

$$P_{d,t_0} = \sum_{l=0}^{2K} \binom{2K}{l} \frac{1}{2^{2K}} F^{-1}_{\chi^2(4K)}(l\lambda_{t_0} + (2K - l)\lambda_0) \qquad (10)$$

The representation of the average probability of detection P_{d,t_0} for different values of K is given in the Figure 5 (worst location for the transition $t_0 = T_I/2$).

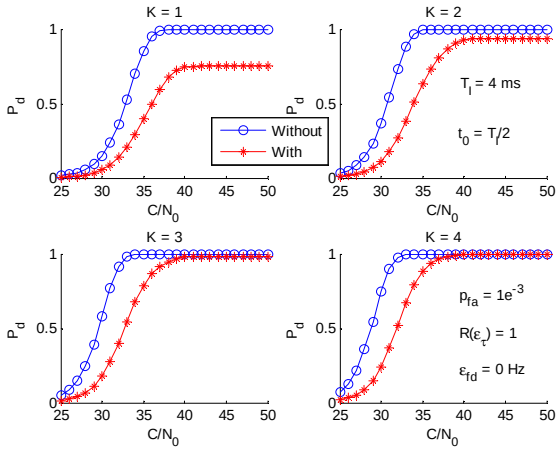

Figure 5: Effect of the data modulation (worst case) on the probability of detection for K=1,2,3,4

What can be seen in Figure 5 is that bit transition greatly affects the probability of detection. It is clear that for $K = 1$, the impact for high C/N_0 is important because a quarter of the probability of detection is null (9). For example, for $K = 4$, for a desired probability of detection of $P_d = 0.95$, the loss is around 5 dB ($C/N_0 = 32$ dBHz without bit transition and $C/N_0 = 37$ dBHz with bit transition). Figure 6 presents the probability of detection for a fixed C/N_0 (27 dBHz) and the conclusion is the same as previous, the probability of detection with a bit transition is significantly lower than the probability of detection without bit transition. In the worst case (t_0 is the center of the integration interval and ε_{f_D}= 0 Hz), one needs more than 3 times more non-coherent summations to reach the same probability of detection of $P_d = 0.95$ ($KT_I = 80$ ms $\rightarrow K = 20$ without bit transition and $KT_I = 264$ ms $\rightarrow K = 66$ with a bit transition exactly in the middle of the coherent integration interval).

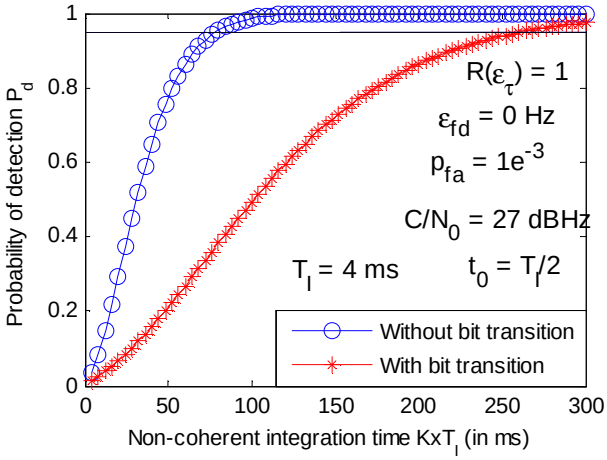

Figure 6: Effect of the data modulation (worst case) on the probability of detection for a C/N_0=27 dBHz

The aim of this section was to study the effect of bit transitions for Galileo E1 OS signal on the probability of detection. The conclusion of this part is that the bit transition has a really bad effect on the probability of detection, in particular for weak Galileo E1 OS signal and for a bit transition in the middle of the integration interval: loss of several dB for a fixed non-coherent integration time and several times more of non-coherent integrations to reach the same objective of probability of detection.

V. Proposed Efficient Galileo E1 OS Initial Acquisition Scheme

A. Presentation of DBZPTI

The DBZP (Double Block Zero Padding) was originally developed for GPS L1 C/A and GPS L1 P(Y) [15] and [16]. The concept of the DBZP relies on the use of partial correlations on a duration equivalent to a few tens of chips (a “block”) and an extensive use of Fourier transforms to speed up the computation of these partial correlations. This acquisition method is considered one of the best for the acquisition of weak signals in terms of number of operations [17].

The theoretical performance of the DBZP was, for the first time, described and analyzed in [4]. In the same paper, a variant method of the DBZP, the DBZPTI (Double Block Zero Padding Transition Insensitive), was presented as a good candidate for Galileo E1 OS signal acquisition to overcome the presence of data bit/secondary code chip transitions, the mathematical model is presented in Appendix B (DBZPTI outputs and execution time of the DBZPTI which gives a numeric application of the splitting in block) and its scheme in Figure 7.

The DBZPTI outputs are reminded here:

$$\begin{aligned} & I_D^2(k) + Q_D^2(k) + I_P^2(k) + Q_P^2(k) \\ = \; & \frac{A^2}{4} M^2 \left(R_{c_{1,D}}^2(\varepsilon_\tau(k)) + R_{c_{1,D}}^2(\varepsilon_\tau(k)) \right) \\ & \times sinc^2\left(\frac{\pi t_i}{M} f_D\right) \frac{\mathrm{sinc}^2(\pi(m - f_D t_i))}{\mathrm{sinc}^2\left(\frac{\pi(m - f_D t_i)}{M}\right)} \end{aligned} \quad (11)$$

The study in [4] shows that the limitation of the DBZPTI is the strong dependence of its performance with respect to the incoming Doppler frequency (degradation of 8 dB on the C/N_0 in the worst Doppler case) because the local carrier does not try to compensate the incoming Doppler frequency as it is the case for the classical acquisition method.

B. DBZPTI Modification for Performance Enhancement

The aim of this section is to remove the limitation of the DBZPTI and reach the same order of degradations as the classical acquisition method in terms of equivalent C/N_0 loss at the correlator output due to the Doppler (around 1 dB).

In the DBZPTI, the number of blocks is defined by the relationship between the the integration time and the Doppler uncertainty $M = \left(f_{D,\max} - f_{D,\min}\right) \times T_I = 80$ where $\left[f_{D,\min}; f_{D,\max}\right] = [-10; 10]$ kHz is the Doppler uncertainty. M corresponds to the number of Doppler bins. The DBZPTI consists in evaluating partial correlation outputs as the partial correlator outputs $\widetilde{I_{D,p}}$ and $\widetilde{Q_{D,p}}$ of the data component:

$$\begin{aligned} & \widetilde{I_{D,p}}(l,k) + \mathrm{i}\widetilde{Q_{D,p}}(l,k) = 2n_{\tilde{I}_p}(l,k) + \frac{A}{2} R_{p,c_{1,D}}(\varepsilon_\tau(k)) \\ & \times sinc\left(\frac{\pi \mathrm{T_I}}{M} f_D\right) exp\left(i2\pi f_D \left(T_0 + \frac{lT_I}{M} + \frac{T_I}{2M}\right) + i\varepsilon_{\phi_0}\right) \end{aligned} \quad (12)$$

Where

- p stands for partial correlation
- l is the partial correlation identification
- ε_τ is the code delay error
- T_0 is the beginning of the integration time
- ε_{ϕ_0} is the phase error at $t = T_0$

The term $sinc\left(\pi \frac{T_I}{M} f_D\right)$ implies a maximum degradation of 4 dB for the maximal expected value of the incoming Doppler frequency. To overcome this problem, it is possible to double the number of blocks M by artificially doubling the theoretical uncertainty Doppler frequency interval. The effect of this manipulation is presented in Figure 8. For $f_D = 10$ kHz (real maximal expected value), the degradation is less than 1 dB (blue line) instead of 4 dB (in dash-dot black line).

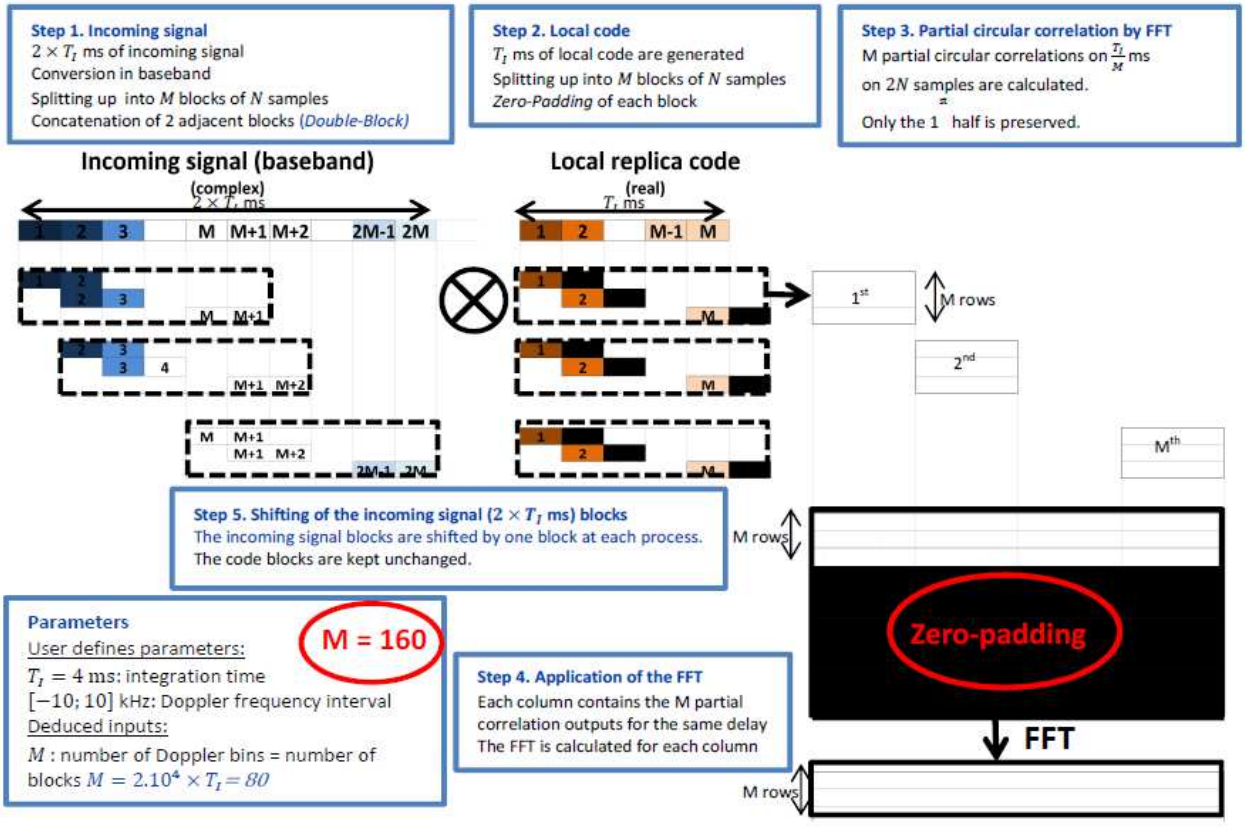

Figure 7: (Optimized) DBZPTI scheme

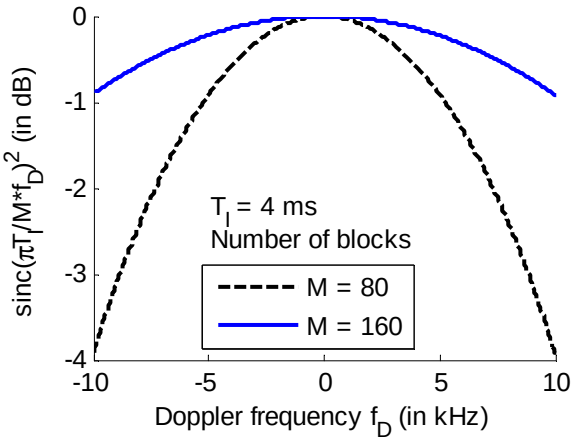

Figure 8: Amplitude of $sinc\left(\pi \frac{T_i}{M} f_D\right)$ versus the incoming Doppler frequency and for 2 values of M

The last step of the DBZPTI uses a Fourier transform on a vector which is the set of partial correlation outputs for a given code delay (with a size equal to the number of blocks M). The FFT result allows determining the incoming Doppler frequency thanks to the term (13). But it implies a maximum degradation of 4 dB (dash-dot black line in Figure 9 for $\beta = 1$) for $f_D = \left(k + \frac{1}{2}\right)\frac{1}{T_I}, k \in [\![-M;M]\!]$:

$$\frac{\mathrm{sinc}(\pi(m - f_D \mathrm{T_I}))}{\mathrm{sinc}\left(\frac{\pi(m - f_D \mathrm{T_I})}{M}\right)} \qquad (13)$$

Where m is the point where the FFT is taken

From (13), it can be understood that the DBZPTI output will present a peak value for the value of m which is the nearest to the incoming Doppler frequency f_D.

To overcome this problem one suggests to zero-pad the vector because the zero-padding is equivalent to oversample the FFT result. Indeed, the more points there are to describe the FFT, the smaller is the gap between $f_D T_I$ and m and the smaller is the degradation.

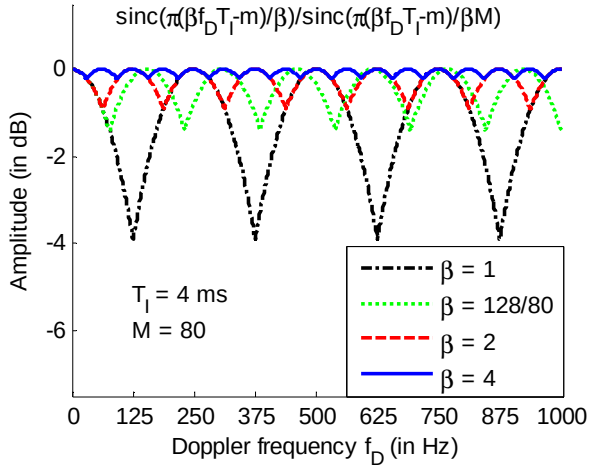

Figure 9: Amplitude of the term (13) versus the incoming Doppler frequency

The development of the expression of the FFT is presented in (14) (the development is in Appendix B) to support the result in Figure 9, for $m = 0 \ldots \beta M - 1$:

$$\begin{aligned} & FFT\left(exp\left(i2\pi f_D\left(T_0 + \frac{lT_I}{M} + \frac{T_I}{2M}\right) + i\varepsilon_{\phi_0}\right)\right) \\ = & \sum_{l=0}^{M-1} e^{\left(i2\pi f_D\left(T_0 + \frac{T_I}{2M}\right) + i\varepsilon_{\phi_0} + 2\pi i f_D \frac{T_I}{M} l\right)} e^{-\frac{2i\pi ml}{\beta M}} \\ = & \mathrm{M} \frac{e^{i\pi f_D(2T_0 + T_I) + i\varepsilon_{\phi_0}}}{e^{\frac{i\pi(M-1)m}{2M}}} \frac{sinc\left(\pi \frac{\beta f_D T_I - m}{\beta}\right)}{sinc\left(\pi \frac{\beta f_D T_I - m}{\beta M}\right)} \end{aligned} \qquad (14)$$

Where βM is the size of the vector on which the FFT is applied

Two sizes of the zero-padded vector are of interest: power of 2 and an integer multiple of the number of blocks to keep a frequential resolution integer divisor of $1/T_I$.

- $\beta M = 128 = 2^7$

To speed up the FFT, the number of added zero allows reaching a size of the vector that is a power of two. The worst degradation is lower than 1.4 dB (dash green line in the Figure 9) for a 128-vector (128 being the next power of 2 after 80).

- $\beta M = 2\mathrm{M}$ (or $\beta M = 4\mathrm{M}$)

The size of the original vector is doubled and in this case, the frequential resolution of the DBZPTI output is also doubled. The worst degradation is for $f_D = \left(\frac{k}{2} + \frac{1}{4}\right)\frac{1}{T_I}, k \in [\![-M;M]\!]$ and only a degradation of 0.9 dB (long dash red line in the Figure 9). The number of lobes (local maxima) is doubled and one over two matches with the original lobes ($\beta = 1$). To have the same number of bins and the same frequency resolution as the original DBZPTI ($1/T_I$), only one over two terms is kept in the FFT result.

For $\beta M = 4M$ (in bold blue line in the Figure 9), the result is more interesting because the worst degradation is 0.19 dB. So this value is retained.

Let us remark that doubling the number of blocks (by artificially doubling the Doppler uncertainty) has not effect on the equation (13) because $sinc\left(\pi \frac{\beta f_D T_I - m}{\beta M}\right)$ is close to 1 (whichever the value of M: 80 or 160).

As explained in this section, with using zero-padding ($\beta = 4$) and doubling the number of blocks (by artificially doubling the Doppler uncertainty), the DBZPTI worst degradation is 1.1 dB which is close to the maximal degradation of the classical acquisition method (0.9 dB).

VI. Comparison of Acquisition Schemes based on the Classical and DBZPTI Initial Acquisition

A. Assessment of execution time of elementary computations

To evaluate the computational efficiency of an algorithm (and/or the acquisition strategy), the

computational load and execution time are good criteria. The number of operations or the execution time of the elementary operations (additions, multiplications, FFT, absolute value…) can be computed. There exists several algorithms to speed up the FFT (such as the Cooley-Tukey algorithm for vectors which size are a power of 2 [17]). In general, the following results are kept for the FFT on a vector of size N:

- If $N = 2^n$, the number of elementary operations (additions and multiplications) is $\mathcal{O}(Nlog_2(N))$.
- Otherwise, with standard FFT algorithms the number of elementary operations is $\mathcal{O}(N^2)$.

Since Matlab uses the FFTW library (an optimized FFT library), it is possible to evaluate the execution time of a FFT (and compared to other elementary operation execution times) for different vector sizes. The averaged results (on 50 000 runs) are presented in Figure 10 and Table 1. The FFT execution time is represented in green in Figure 10 and it greatly varies with the size of the vectors. So during the computational load evaluation of both acquisition strategies, the execution time (based on elementary operation execution times) is preferred over the number of operations because there are several optimized FFT algorithms -for several vectors which size is not a power of 2, the execution time of the FFT is comparable to this of vector of size power of 2- and the number of operations (additions and multiplications) of each one is unknown.

Table 1: Execution time (10^{-5} seconds) of complex elementary operations for specific size of vectors with Matlab

Size of vector	FFT	Addition	Product	Absolute value
1	0.071	0.084	0.049	0.052
80	0.297	0.08	0.088	0.469
128	0.392	0.089	0.113	0.718
161	0.856	0.1	0.129	0.883
640	1.614	0.197	0.366	3.329
1024	2.62	0.281	0.559	5.41
2048	5.588	0.533	1.103	11.161
81920	439.318	61.656	57.253	442.733

Where

- 80 is the number of the original DBZPTI
- 128 is the next power of 2 after 80
- 161 is the number of Doppler bins in the classical acquisition method
- 640 is the size of the vector on which is applied the last FFT in the modified DBZPTI
- 1024 is the size of the doubled blocks in the modified DBZPTI
- 2048 is the size of the doubled blocks in the original DBZPTI
- 81920 is the size of 4 ms of sampled signal

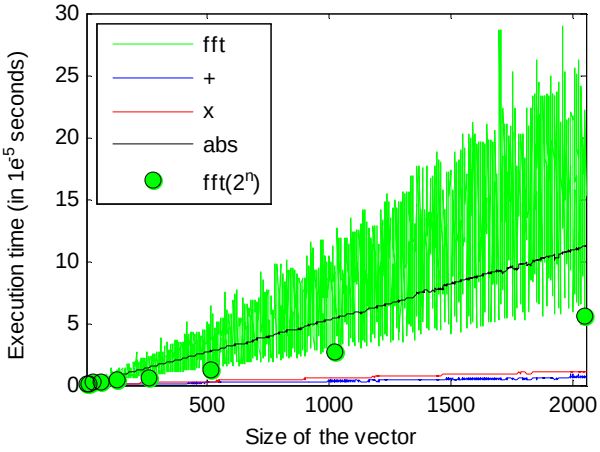

Figure 10: Execution time of elementary operations

As seen with Figure 10 and Table 1, the most computational expensive operations are the FFT and the absolute value, their executions need between 6 and 7 times more than the execution time of an addition or product.

This section serves to understand what are the computational cost elementary operations and their relatively cost in function of the size of the vectors. Matlab simulations give an order of idea of the computational cost of the elementary operations and acquisition strategies. However, the expected execution time of the acquisition strategies, developed in C++, is obviously lesser.

B. Consideration about the Verification Step

Firstly, let us remark that the bit transition is not considered in the verification step because the initial acquisition gives a rough estimation of the code delay and thus the verification step takes into account the correct alignment.

In the acquisition process, different strategies can be adopted in order to explore the search with different speeds and accuracies [19]. It is thus necessary to thoroughly choose the way the bins are selected after the initial acquisition, and the way these bins are then verified. The verification step can be full (the whole correlation matrix is verified) or partial verification (only a small number of bins is verified). Whatever the strategy, the order of the verified bins should be established. Two strategies can be considered [19]:

- Maximum:

Only the bin(s) corresponding to the maximum (or the first maxima) of the acquisition detector is (are) verified.

- Serial:

Once a value of the correlation matrix is obtained and crosses the acquisition threshold, it is verified.

It is clear that the best strategy of verification in terms of computation load is the first one which consists in verifying a single or small number of maxima. But the amplitude of the detector for the “right bin” should be compared to the amplitude for the other

bins to determine how many bins should be verified id est the position of the amplitude of the right bin regarding to the amplitude of the other bins.

To determine the ordered position of the amplitude of the detector of the right bin, an acquisition matrix is simulated over N bins with Matlab. The simulated incoming Doppler frequency is within$[-10; 10]$ kHz. $N-1$ bins are randomly distributed according to a $\chi^2(4K)$ and 1 bin (the "right bin") is distributed according to a $\chi^2(4K, \lambda)$ where λ is the non-centrality parameter.Only the bins overcrossing the threshold defined by the statistic model are kept (false alarms and potentially the right bin). The bins are ordered by decreasing amplitude. After that, the ranking of the right bin with respect to amplitude is extracted versus the number of non-coherent summations. The results of the simulations for the two acquisition strategies are given in following sections.

C. Choice of Parameters and Performance for the DBZPTI-based Acquisition Scheme

Knowing that the acquisition detector is a χ^2 distribution with $4K$ degrees of freedom, it is easy to determine the required number of non-coherent integrations to reach the objectives. For a fixed probability of false alarm of 10^{-3} (in general it is the retained value) and C/N_0 of 27 dBHz, between 26 and 40 summations are needed. As explained in previous section, the Figure 11 presents the statistic position of the amplitude of the acquisition detector for the right bin with regards to the amplitude of the false alarms. The size of the acquisition matrix is $655360 = 80 \times 81920$ (number of kept blocks times the number of samples for 4 ms) and there are around 6550 false alarms. Figure 11 shows that for a sufficient high number of non-coherent summations, only several bins have to be verified (and not the whole acquisition matrix).

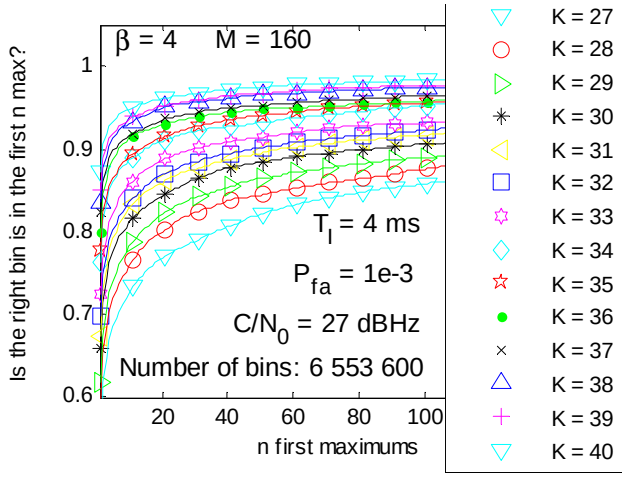

Figure 11: Position of the amplitude of the right bin for the DBZPTI

Let us evaluate the probability of detection of the DBZPTI-based acquisition strategy and noted as P_d. It is the product of the probability of detection of the DBZPTI noted as $P_{d,DBZPTI}$ and of the verification step noted as $P_{d,MofN}$ (15) because the two events are independents.

$$\begin{aligned} P_d &= P_{H_1}\left(C_{DBZPTI} \bigcap C_{MofN}\right) \\ &= P_{H_1}(C_{DBZPTI}) \times P_{H_1}(C_{MofN}) \\ &= P_{d,DBZPTI} \times P_{d,MofN} \end{aligned} \quad (15)$$

Where

- s stands for $DBZPTI$ acquisition step or for $MofN$ acquisition step
- C_s is the event $\{T_s > Th_s\}$, the acquisition criterion is satisfied
- T_s is the acquisition detector
- Th_s is the acquisition threshold

To reach a probability of detection greather than 0.9 implies that the probabilities of detection for the two steps (DBZPTI and M of N) should be around 0.95.

The probability of false alarm of the acquisition process is a little bit different due to the fact that only a few false alarms are verified.

$$\begin{aligned} P_{fa} &= P_{H_0}\left(\left(C_{DBZPTI} \bigcap M_n\right) \bigcap C_{MofN}\right) \\ &= P_{H_0}(M_n | C_{DBZPTI}) P_{H_0}(C_{DBZPTI}) \times P_{H_0}(C_{MofN}) \\ &= \frac{n}{N_v} \times P_{fa,DBZPTI} \times P_{fa,MofN} \end{aligned} \quad (16)$$

Where

- M_n corresponds to the event: the amplitude of the acquisition detector for the DBZPTI of this false alarm is among the n highest i.e. this false alarm is among the verified bins
- N_v is the number of verified bins by the M of N acquisition step

After several considerations on the M of N acquisition step, based on the binomial distribution, a rough estimation of the parameters can be provided:

- What is the best allocation between $P_{fa,DBZPTI}$ and $P_{fa,MofN}$, and between $P_{d,DBZPTI}$ and $P_{d,MofN}$ to reach the objectives?
- How many non-coherent summations are needed to obtain the minimal value of P_d?
- What is the best choice for M and N for the M of N acquisition step?

The choice of the exact value of the parameters $(K, M, N\, p_{fa}, p_d)$ is done regarding to the overall objective of probability of detection. For different values of parameters leading to the same probability of detection, the execution time of the acquisition process is the second criterion. Indeed, a compromise should be done between the two acquisition steps (DBZPTI and verification step) because the number of verified bins by the verification step results of the probability of false alarm of the DBZPTI and of the position of the amplitude of the right bin (depending on the number of non-coherent summations).

The execution of one non-coherent summation for the DBZPTI costs around 7 seconds (Appendix B) and the execution time of the M of N acquisition step to verify one bin is 1.5 seconds (Appendix C). In conclusion, it is relatively expensive to verify bins, so the number of bins to verify should be very small.

[12] gives the best combination for M and N for the M of N acquisition, it is 5 of 8. The Matlab simulations confirm this result for the case of interest. So, with 38 non-coherent summations for the DBZPTI acquisition step and 8 non-coherent summations for the M of N acquisition step, the probability of detection (for any C/N_0 equal to or higher than 27 dBHz, whichever the incoming Doppler frequency and the code delay) is of 90%. Indeed,

- $P_{d,DBZPTI} = 0.93$ and the amplitude of the right bin is in the 10 first maxima
- $P_{d,MofN} = 0.97 = \sum_{k=5}^{8} \binom{8}{k} p_d^k (1-p_d)^{8-k}$ with $p_d = 0.84$ the probability of detection for one detector of the M of N acquisition step
- $P_{fa,MofN} = 0.06 = \sum_{k=5}^{8} \binom{8}{k} p_{fa}^k (1-p_{fa})^{8-k}$ with $p_{fa} = 0.3$ the probability of false alarm for one detector of the M of N acquisition step
- $n = 10$ is the number of verified bins given by the 10 first maxima of the DBZPTI acquisition matrix

In conclusion, the DBZPTI-based acquisition strategy needs 38 non-coherent summations to reach the probability of detection of 0.9.

D. Choice of Parameters and Performance for the Classical Acquisition Scheme

As seen in section IV.B (in particular with Figure 5), in presence of a bit transition (at the worst location), the number of non-coherent summations is greater than 66 for a Doppler frequency error as minimal as possible to reach a probability of detection greater than 0.95.

A Matlab simulation was run to determine the position of the amplitude of the right bin, its results are presented in Figure 12.

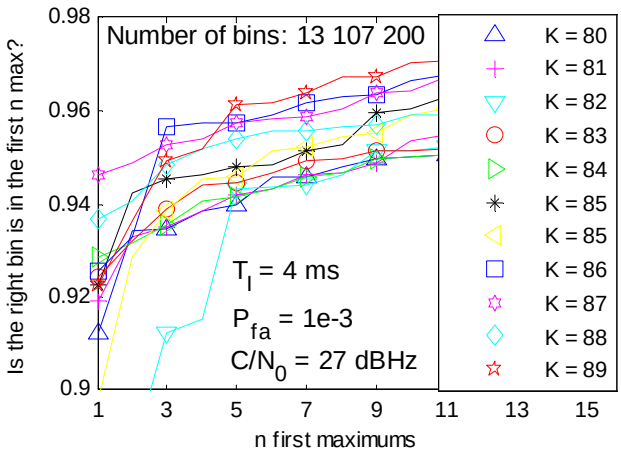

Figure 12: Position of the amplitude of the right bin for the classical acquisition method

The probability of false alarm of the acquisition strategy based on the classical acquisition method (CAM) should be the same as this for the acquisition strategy based on the DBZPTI. However, the number of false alarms crossing the threshold is doubled by 2 ($N_v = 13108 = P_{fa,CAM} \times 13108$) so the number of verified bins n should be divided by 2. Thus, the number of non-coherent summations for the classical acquisition method is 82 (in this way, the amplitude of the right bin is in the 5 first maxima of the classical acquisition matrix).

At the end, the performance of this acquisition process can be evaluated:

- $P_{d,CAM} = 0.93$ and the amplitude of the right bin is in the 5 first maxima
- $P_{d,MofN} = 0.97 = \sum_{k=5}^{8} \binom{8}{k} p_d^k (1-p_d)^{8-k}$ with $p_d = 0.84$ the probability of detection for one detector of the M of N acquisition step
- $P_{fa,MofN} = 0.06 = \sum_{k=5}^{8} \binom{8}{k} p_{fa}^k (1-p_{fa})^{8-k}$ with $p_{fa} = 0.3$ the probability of false alarm for one detector of the M of N acquisition step
- $n = 5$ is the number of verified bins given by the 5 first maxima of the classical acquisition matrix

In conclusion, the acquisition strategy based on the clasical acquisition needs 82 non-coherent summations to reach the probability of detection of 0.9.

E. Comparison of Execution Time

The averaged execution (with Matlab) of the acquisition strategies can be computed.

For the DBZPTI-based acquisition strategy: 38 non-coherent summations are needed for the DBZPTI step, it leads to 250 seconds. Moreover, the verification of 10 bins leads to an execution time of 15 seconds. Then, the total amount of time for the DBZPTI-based acquisition strategy is 266 seconds.

For the classical acquisition-based acquisition strategy: 82 non-coherent summations are needed for the classical acquisition step, it leads to 405 seconds. Moreover, the verification of 5 bins leads to an execution time of 7 seconds. Then, the total amount of time for the DBZPTI-based acquisition strategy is 413 seconds.

In conclusion, the execution time of the DBZPTI-based acquisition strategy (based on Matlab simulations and estimations) is really lower than the other acquisition strategy. It is reasonable to think that at least this ratio (1.5), will be kept on C++ implantation. Moreover, one of the advantage of the DBZPTI is that lot of FFTs can be done in a parallel way leading to reduce the averaged execution time on a multi-cores platform.

To reduce the execution time of whatever the acquisition strategy, it is possible to subsample the signal. Indeed, with a sampling frequency of $f_s = 20.48$ MHz, around 20 samples describe one chip, so it is possible to keep one over three samples for

example. But this causes considerable degradations (around 2.5 dB) which can be a problem for the acquisition of weak signals.

VII. Conclusions

This paper presents two different acquisition strategies for the acquisition of Galileo E1 OS signals which are based on two acquisition methods: the optimized DBZPTI (which is transition insensitive) and the classical acquisition method. The objective is to perform the acquisition of signals at 27 dBHz with a high probability of detection (90%).

This paper highlights the high interest of transition insensitivity for a Galileo E1 OS signal acquisition method. Indeed, the presented study of the effect of the data modulation presents the degradation of a bit transition -data and/or secondary code- (loss of several dB depending on the non-coherent integration time, the location of the bit transition and the frequency error). The last sections establish the two acquisition strategies allowing the acquisition of weak Galileo E1 OS signals (27 dBHz) 90% of the time (all conditions).

The execution time of elementary operations -FFT being one of the most critical- is evaluated to determine the averaged execution time of each acquisition strategies: with Matlab, 267 seconds for the acquisition strategy based on the DBZPTI and 413 seconds for the acquisition strategy based on the classical acquisition method. This represents a duration 1.5 times longer than the acquisition strategy based on the DBZTI for the same performance (overall probability of detection $P_d = 0.9$ and of false alarm $P_{fa} = 10^{-7}$). Due to its insensitivity of bit transition, the acquisition strategy based on the DBZPTI appears as the good one.

Due to the high number of non-coherent summations, it can be interesting to study the degradation of the Doppler frequency on the code frequency for the two acquisition methods. [20] for example begins this study, developing a variant of the DBZP.

VIII. References

[1] GPS World, “Receiver Survey 2011, sponsored by Novatel,” *GPS World January 2011*, Jan-2011.

[2] GPS World, “Receiver Survey 2012, sponsored by Novatel,” *GPS World January 2012*, Jan-2012.

[3] GPS World, “Receiver Survey 2013, sponsored by Novatel,” *GPS World January 2013*, Jan-2013.

[4] M. Foucras, O. Julien, C. Macabiau, and B. Ekambi, “A Novel Computationally Efficient Galileo E1 OS Acquisition Method for GNSS Software Receiver,” in *ION GNSS 2012*, Nashville, TN, 2012.

[5] European Commission, “European GNSS (Galileo) Open Service - Signal-in -Space, Interface Control Document Issue 1.” Feb-2010.

[6] G. N. S. S. Navigation, “Sx -NSR,” *Interfaces*, no. May, 2011.

[7] G. E. Corazza, C. Palestini, R. Pedone, and M. Villanti, “Galileo primary code acquisition based on multi-hypothesis secondary code ambiguity elimination,” *Int. J. Satell. Commun. Netw.*, vol. 24, no. 2, pp. 153–167, 2006.

[8] F. Bastide, “Analysis of the Feasibility and Interests of Galileo E5a/E5b and GPS L5 for Use with Civil Aviation,” PhD., Institut National Polytechnique de Toulouse, Toulouse, France, 2004.

[9] D. Borio and L. Lo Presti, “Data and Pilot Combining for Composite GNSS Signal Acquisition,” *Int. J. Navig. Obs.*, vol. 2008, pp. 1–12, 2008.

[10] E. Pajala, E. S. Lohan, and M. Renfors, “CFAR detectors for hybrid-search acquisition of Galileo signals,” in *Technology*, Munich, Germany, 2005.

[11] E. D. Kaplan and C. Hegarty, *Understanding GPS: Principles and Applications*, Artech House. 1997.

[12] P. W. Ward, “GPS receiver search techniques,” in *Position Location and Navigation Symposium (IEEE)*, 1996, pp. 604–611.

[13] E. D. Kaplan and C. Hegarty, *Understanding GPS: Principles and Applications*. Artech House, 2005.

[14] C. O’Driscoll, “Performance Analysis of the Parallel Acquisition of Weak GPS Signals,” PhD, National University of Ireland, 2007.

[15] D. M. Lin, J. B. Y. Tsui, and T. Howell, “Direct P(Y) code acquisition algorithm for software GPS receivers,” in *ION GPS 99*, Nashville, TN, 1999.

[16] D. M. Lin and J. B. Y. Tsui, “Acquisition schemes for software GPS receiver,” in *ION GPS 1998*, Nasville, TN, 1998.

[17] D. Lin and J. B. Y. Tsui, “Comparison of acquisition methods for software GPS receiver,” in *ION GPS 2000*, Salt Lake City, UT, 2000.

[18] J. W. Cooley and J. W. Tukey, “An algorithm for the machine computation of the complex Fourier series,” *Math Comput.*, vol. 19, pp. 297–301, Apr. 1965.

[19] D. Borio, L. Camoriano, and L. Lo Presti, “Impact of GPS acquisition strategy on decision

probabilities," *Aerosp. Electron. Syst. Ieee Trans.*, vol. 44, no. 3, 2008.
[20] N. I. Ziedan, *GNSS receivers for weak signals*. Artech House, 2006.
[21] B. Chibout, "Application of indoor and urban GNSS localisation techniques to space navigation," PhD, INP Toulouse, France, 2008.

IX. APPENDICES

A. Appendix A: Classical acquisition method

1) Correlator outputs for the non-coherent combining method

The correlation outputs for the classical method are largely described [9] and given a reminder here:

$$\begin{aligned} I_D(k) &\approx \frac{A}{2} R_{c_{1,D}}(\varepsilon_\tau(k)) sinc(\pi \varepsilon_{f_D} t_i) cos(\varepsilon_\phi) + n_{I_D}(k) \\ Q_D(k) &\approx \frac{A}{2} R_{c_{1,D}}(\varepsilon_\tau(k)) sinc(\pi \varepsilon_{f_D} t_i) sin(\varepsilon_\phi) + n_{I_D}(k) \\ I_P(k) &\approx \frac{A}{2} R_{c_{1,P}}(\varepsilon_\tau(k)) sinc(\pi \varepsilon_{f_D} t_i) cos(\varepsilon_\phi) + n_{I_P}(k) \\ Q_P(k) &\approx \frac{A}{2} R_{c_{1,P}}(\varepsilon_\tau(k)) sinc(\pi \varepsilon_{f_D} t_i) sin(\varepsilon_\phi) + n_{I_P}(k) \end{aligned}$$

Where $\varepsilon_\phi = \pi \varepsilon_{f_d} t_i + \varepsilon_{\phi_0}$ is the error on the phase

The variance of these correlator outputs are:

$$var(I_D(k)) = var(Q_D(k)) = var(I_P(k)) = var(Q_P(k)) = \sigma^2 = \frac{N_0}{4t_i}$$

The acquisition detector for this method is:

$$T = \sum_{k=1}^{K} I_D^2(k) + Q_D^2(k) + I_P^2(k) + Q_P^2(k)$$

2) Statistic model

The performance study follows the Neyman-Pearson's approach that is based on the hypothesis test [21].

Let us assume that the useful signal is absent and there is only noise. Because the noise is assumed as white and Gaussian, the normalized acquisition detector T_0/σ^2, in this case, is a χ^2 distribution with $4K$ degrees of freedom. The probability of false alarm P_{fa} is the probability that the signal is declared present (the threshold is crossed) whereas only noise is present.

$$P_{fa} = P_{H_0}(H_1) = P_{H_0}(T_0 > T_h)$$

So the threshold T_h can easily be deduced for a predefined value of probability of false alarm.

Let us now assume that the useful signal is present. The normalized acquisition detector, T_1/σ^2 is a non-central χ^2 distribution with $4K$ degrees of freedom and a non-centrality parameter λ. Details of the computation of λ are given. Firstly, the mean of the in-phase data correlator output is evaluated:

$$\lambda_{k,I_D} = E\left[\frac{I_D(k)}{\sqrt{\sigma^2}}\right] = \frac{1}{\sqrt{\sigma^2}} \times \frac{A}{2} R_{c_{1,D}}(\varepsilon_\tau(k)) sinc(\pi \varepsilon_{f_D} t_i) cos(\varepsilon_\phi)$$

Secondly, the non-centrality parameter for one component (the data component for example here) is evaluated.

$$\lambda_D = \sum_{k=1}^{K} \left(\lambda_{k,I_D}^2 + \lambda_{k,Q_D}^2\right)$$

$$= \sum_{k=1}^{K} \left(\frac{1}{\sigma^2} \times \frac{A^2}{4} R_{c_{1,D}}^2 \left(\varepsilon_\tau(k)\right) sinc^2\left(\pi \varepsilon_{f_D} t_i\right) \right)$$

$$= \frac{A^2}{N_0} t_i K R_{c_{1,D}}^2 \left(\varepsilon_\tau(k)\right) sinc^2\left(\pi \varepsilon_{f_D} t_i\right)$$

Finally, the non-centrality parameter is:

$$\lambda = \lambda_D + \lambda_P$$

$$= \frac{A^2}{N_0} t_i K \left[R_{c_{1,D}}^2 \left(\varepsilon_\tau(k)\right) + R_{c_{1,P}}^2 \left(\varepsilon_\tau(k)\right)\right] sinc^2\left(\pi \varepsilon_{f_D} t_i\right)$$

The conclusion of the statistic model is:

$$\frac{T}{\sigma_I^2} \sim \begin{cases} \chi^2(4M), H0: useful\ sigal\ not\ present \\ \chi^2(4M, \lambda), H1: useful\ sigal\ present \end{cases}$$

3) Execution time

The execution time of the classical acquisition method is described here.

Table 2: Detailled execution time of the classical acquisition method technique (in seconds)

Operations	Size of vectors (N) Size of the matrix	Unity execution time	Number of repeated times			Execution time
			For 1 integration	Non-cohe. Summation	Pilot/Dta	
Multiplication by the local carrier	81920	5,73E-04	161	82		7,4E+00
fft of the signal	81920	4,39E-03	161	82		5,7E+01
fft of the code	81920	2,10E-03	1	1	2	4,2E-03
Conjuguate of the fft	81920	5,62E-03	1	1	2	1,1E-02
Multiplication of the ffts	81920	5,73E-04	161	82	2	1,5E+01
ifft	81920	5,62E-03	161	82	2	1,4E+02
Normalize by 1/N	81920	4,76E-04	161	80	2	1,2E+01
Squared absolute value	1,3E+07	8,23E-01		80	2	1,3E+02
Non-coherent summations	1,3E+07	1,19E-01		79	3	2,8E+01
TOTAL						405

Where

- 81920: size of the $T_I = 4\ \mathrm{ms}$ of signal (due to sampling frequency of $f_s = 20.48\ \mathrm{MHz}$)
- 161: number of Doppler bins
- 13189120= 81920×161: size of the acquisition matrix
- 80: number of non-coherent summations
- 2: done for data and pilot spreading codes

B. Appendix B: DBZPTI acquisition method

1) Choice of the spreading code sequences

In [4], the locally spreading code sequences weredifferent to this paper. Indeed, some acquisition methods, as the coherent combining of the data and pilot components is based on sign recovery [9]. So, to overcome the problem of the two unknown bits, the received signal is correlated with both equivalent spreading code sequences (sum and difference of the data and pilot spreading codes: $c_{1,D}(t)p_{CBOC,D}(t) + \alpha c_{1,P}(t)p_{CBOC,P}(t)$ where $\alpha = \pm 1$). Thus, only one of the two equivalent code sequences has the same sign as the incoming signal, giving a maximum correlation while the other should be dominated by noise. A work has been done to study that for low C/N_0 the choice of the kept correlation matrix (this giving the maximum correlation) does not correspond to the matrix given the maximum correlation value for the right bin, this means that it is the noise which determines the kept matrix and one time over two, the equivalent code sequence giving the maximum correlation has not the same sign as the incoming signal. Figure 13 shows that the probability that the amplitude of the acquisition detector of the right bin maximizes the detector is null for a C/N_0 of 27 dBHz. It is why this choice of this local spreading code sequences (sum and difference of the data and pilot spreading code) is no longer used for the acquisition of weak signal and the signal is correlated independently with the local data and spreading codes.

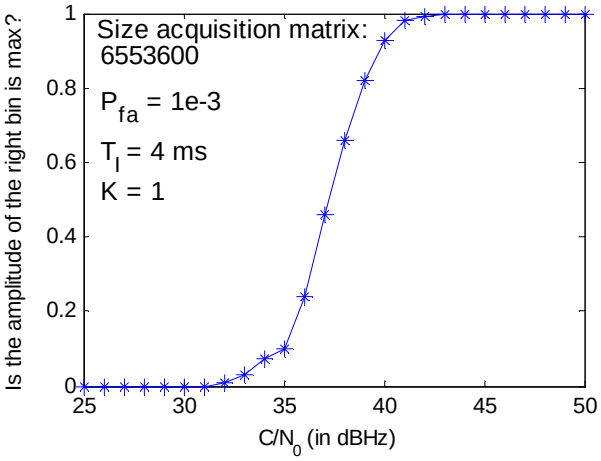

Figure 13: Is the amplitude of the right bin the maximum?

2) DBZPTI outputs

The partial correlation outputs computed in the DBZPTI are given here, they are two partial correlation outputs per component

$$\widetilde{I_{x,p}}(l,k) = n_{\widetilde{I_p}}(l,k) +$$
$$\frac{A}{2}R_{p,c_{1,x}}(\varepsilon_\tau(k))sinc\left(\frac{\pi t_i}{M}f_D\right)cos\left(2\pi f_D\left(t_0+\frac{lt_i}{M}+\frac{t_i}{2M}\right)+\varepsilon_{\phi_0}\right)$$
$$\widetilde{Q_{x,p}}(l,k) = n_{\widetilde{Q_p}}(l,k) +$$
$$\frac{A}{2}R_{p,c_{1,x}}(\varepsilon_\tau(k))sinc\left(\pi f_D\frac{t_i}{M}\right)sin\left(2\pi f_D\left(t_0+\frac{lt_i}{M}+\frac{t_i}{2M}\right)+\varepsilon_{\phi_0}\right)$$

Where x stands for D for data and P for pilot

At the end, the DBZPTI outputs are:

$$I_x^2(k)+Q_x^2(k) = \left|fft\left(\widetilde{I_{x,p}}(l,k)+\mathrm{i}\times\widetilde{Q_{x,p}}(l,k)\right)\right|^2$$
$$= \frac{A^2}{4}M^2R_{c_{1,x}}^2(\varepsilon_\tau(k))sinc^2\left(\frac{\pi t_i}{M}f_D\right)\frac{\mathrm{sinc}^2(\pi(m-f_Dt_i))}{\mathrm{sinc}^2\left(\frac{\pi(m-f_Dt_i)}{M}\right)}$$

Let us evaluate the variance. The variance of the partial correlator is:

$$\sigma_{\widetilde{I_p}}^2 = var\left(\widetilde{I_{D,p}}(l,k)\right) = \frac{N_0}{4\frac{t_i}{M}}$$

And the variance of the DBZPTI output is:

$$\sigma_I^2 = var\left(I_D(k)\right) = \frac{N_0M^2}{4t_i}$$

The acquisition detector is:

$$T = \sum_{k=1}^{K} I_D^2(k)+Q_D^2(k)+I_P^2(k)+Q_P^2(k)$$

3) Statistic model

With the same approach as for the classical acquisition method, the acquisition detector is:

$$\frac{T}{\sigma_I^2}\sim\begin{cases}\chi^2(4M), H0: useful\ sigal\ not\ present\\ \chi^2(4M,\lambda), H1: useful\ sigal\ present\end{cases}$$

Where

$$\lambda = \sum_{k=1}^{K}\left(\lambda_{k,I_D}^2+\lambda_{k,Q_D}^2+\lambda_{k,I_P}^2+\lambda_{k,Q_P}^2\right) = \lambda_D+\lambda_P$$
$$= \frac{A^2}{N_0}Kt_i\left(+\frac{R_{c_{1,D}}^2(\varepsilon_\tau(k))}{R_{c_{1,P}}^2(\varepsilon_\tau(k))}\right)sinc^2\left(\frac{\pi t_i}{M}f_D\right)\left(\frac{sinc(\pi(m-f_Dt_i))}{sinc\left(\frac{\pi(m-f_Dt_i)}{M}\right)}\right)^2$$

4) Development of the last FFT

The development of the last FFT of the DBZPTI (on the partial correlator outputs for the same code delay) is presented here.

$$fft\left(exp\left(\mathrm{i}2\pi f_D\left(\mathrm{T_0}+\frac{l\mathrm{T_I}}{M}+\frac{\mathrm{T_I}}{2M}\right)+i\varepsilon_{\phi_0}\right)\right)\left(m_{m=0\dots\beta M-1}\right)$$
$$= \sum_{l=0}^{M-1} exp\left(\mathrm{i}2\pi f_D\left(\mathrm{T_0}+\frac{\mathrm{T_I}}{2M}\right)+\varepsilon_{\phi_0}+2\pi i f_D\frac{\mathrm{T_I}}{M}l\right)e^{-\frac{2i\pi ml}{\beta M}}$$
$$= e^{2i\pi f_D\left(\mathrm{T_0}+\frac{\mathrm{T_I}}{2M}\right)+i\varepsilon_{\phi_0}}\sum_{l=0}^{M-1}e^{i2\pi f_D\frac{\mathrm{T_I}}{M}l}e^{-\frac{2i\pi ml}{\beta M}}$$
$$= e^{2i\pi f_D\left(\mathrm{T_0}+\frac{t_i}{2M}\right)+i\varepsilon_{\phi_0}}\sum_{l=0}^{M-1}e^{2i\pi\left(f_D\frac{\mathrm{T_I}}{M}-\frac{m}{\beta M}\right)l}$$
$$= e^{2i\pi f_D\left(\mathrm{T_0}+\frac{t_i}{2M}\right)+i\varepsilon_{\phi_0}}\sum_{l=0}^{M-1}e^{2i\pi\left(\frac{\beta f_D\mathrm{T_I}-m}{\beta M}\right)l}$$
$$= \mathrm{M}e^{-\frac{i\pi(M-1)m}{2M}}e^{i\pi f_D(2\mathrm{T_0}+\mathrm{T_I})+i\varepsilon_{\phi_0}}\frac{sinc\left(\pi\frac{\beta f_D\mathrm{T_I}-m}{\beta}\right)}{sinc\left(\pi\frac{\beta f_D\mathrm{T_I}-m}{\beta M}\right)}$$

5) Execution time of the DBZPTI

The execution time of the DBZPTI method is described in the Table 3.

Table 3: Detailled execution time of the DBZPTI technique (in seconds)

	Operations	Size of vectors (N) Size of the matrix	Unity execution time	Number of repeated times			Execution time
				For 1 integration	Non-cohe. Summation	Pilot/Data	
Step 1	Multiplication by the local carrier	81920	5,73E-04	1	38		0
Step 3	fft of the signal	1024	2,01E+01	25600	38		25
	fft of the code	1024	2,51E-03	160	1	2	0
	Conjuguate of the fft	1024	5,34E-04	160	1	2	0
	Multiplication of the ffts	1024	4,29E+00	25600	38	2	11
	ifft	1024	2,56E+01	25600	38	2	65
	Normalize by 1/N	1024	4,76E+00	25600	38	2	12
Step 4	Last fft	640	3,97E+01	81920		2	100
	Squared absolute value	7,E+06	1,20E+01		38	2	30
	Non-coherent summations	7,E+06	1,59E+00		37	3	6
TOTAL							**250**

Where

- 81920: size of the $T_I = 4\,\text{ms}$ of signal (due to sampling frequency of $f_s = 20.48\,\text{MHz}$)
- 160: number of blocks (doubled)
- 1024= $\frac{81920}{160} \times 2$: number of samples per double-sized block
- 640 = 160x4 size of the vector for the last FFT ($\beta = 4$)
- 6553600 (noted as "7e+06") $= 80 \times 81920$: size of the DBZPTI output matrix
- 25600 = 160x160 (for all blocks of 1 cycle and for all cycles)
- 38: number of non-coherent summations
- 2: done for data and pilot spreading codes

C. Appendix C: Verification step

1) M of N mathematical model

The M of N uses the classical acquisition method to compute the correlator outputs. However, the FFT is not used (to speed up the correlation) because its use is more expensive in execution time. So the received signal is multiplied by a local carrier (including the estimate of the Doppler frequency) and by a local code replica, after that the integration and dump process is done. The code delay bin length is 1/6 chip (the authorized maximal degradation is 2.5dB for 1/12 chip –the same as for GPS L1 C/A for code bin length of ½ chip) and the Doppler frequency bin is of size $1/2T_I$ which implies a maximal Doppler frequency error of $1/4T_I$.

2) Execution time of the M of N acquisition technique

The execution time of the M of N is described here.

Table 4: Detailled execution time of the M of N technique (in seconds)

Operations	Size of vectors (N)	Unity execution time	Number of repeated times			Execution time
			Non-coherent Summation	Pilot/Data	Number of surrounding bins	
Multiplication by the code	81920	0,00057	8		10	4,6E-01
Summation	81920	0,00062	8	2	10	9,2E-01
Squared absolute value	1	5,2E-07	8	2	10	9,9E-01
Non-coherent summations	1	6,3E-07	7	3	10	8,3E-04
TOTAL						**1.53**

Where

- 81920: size of the $T_I = 4\,\text{ms}$ of signal (due to sampling frequency of $f_s = 20.48\,\text{MHz}$)
- 10: number of verified bins (immediate surrounding bins)
- 8: number of non-coherent summations
- 2: done for data and pilot spreading codes

The total of the execution time should be multiplied by the mean of M and N to evaluate the averaged execution time of the M of N acquisition step.

D. Appendix D: Correlator output in presence of a bit transition

Without loss of generality, let us assume that before $t_0 \in [kT_I; (k+1)T_I]$, the value of the bit (data bit or secondary code bit) is 1 and after is is -1:

$$
\begin{aligned}
& I_{t_0}(k) \\
= & \frac{1}{T_I}\left(\begin{array}{l} \int_{kT_I}^{t_0} (1) \times cos\left(2\pi\varepsilon_{f_D} t + \varepsilon_{\phi_0}\right) dt \\ + \int_{t_0}^{(k+1)T_I} (-1) \times cos\left(2\pi\varepsilon_{f_D} t + \varepsilon_{\phi_0}\right) dt \end{array} \right) \\
= & \frac{1}{T_I}\left[\frac{1}{2\pi\varepsilon_{f_D}} sin\left(2\pi\varepsilon_{f_D} t + \varepsilon_{\phi_0}\right)\right]_{kT_I}^{t_0} \\
& -\frac{1}{T_I}\left[\frac{1}{2\pi\varepsilon_{f_D}} sin\left(2\pi\varepsilon_{f_D} t + \varepsilon_{\phi_0}\right)\right]_{t_0}^{(k+1)T_I} \\
= & \frac{1}{2\pi\varepsilon_{f_D} T_I}\left(\begin{array}{c} \left(sin\left(2\pi\varepsilon_{f_D} t_0 + \varepsilon_{\phi_0}\right) - sin\left(2\pi\varepsilon_{f_D} kT_I + \varepsilon_{\phi_0}\right)\right) \\ \left(sin\left(2\pi\varepsilon_{f_D}(k+1)T_I + \varepsilon_{\phi_0}\right) - sin\left(2\pi\varepsilon_{f_D} t_0 + \varepsilon_{\phi_0}\right)\right) \end{array} \right) \\
= & \frac{1}{2\pi\varepsilon_{f_D} T_I}\left(\begin{array}{c} sin\left(2\pi\varepsilon_{f_D} t_0 + \varepsilon_{\phi_0}\right) + sin\left(2\pi\varepsilon_{f_D} t_0 + \varepsilon_{\phi_0}\right) \\ -sin\left(2\pi\varepsilon_{f_D} kT_I + \varepsilon_{\phi_0}\right) - sin\left(2\pi\varepsilon_{f_D}(k+1)T_I + \varepsilon_{\phi_0}\right) \end{array} \right) \\
= & \frac{1}{2\pi\varepsilon_{f_D} T_I}\left(\begin{array}{c} -\left(sin\left(2\pi\varepsilon_{f_D} kT_I + \varepsilon_{\phi_0}\right) + sin\left(2\pi\varepsilon_{f_D}(k+1)T_I + \varepsilon_{\phi_0}\right)\right) \\ +2sin\left(2\pi\varepsilon_{f_D} t_0 + \varepsilon_{\phi_0}\right) \end{array} \right)
\end{aligned}
$$

And after trigonometrical consideration, the in-phase correlator output becomes:

$$
\begin{aligned}
& I_{t_0}(k) \\
= & \frac{2}{2\pi\varepsilon_{f_D} T_I}\left(\begin{array}{c} -sin\left(\frac{2\pi\varepsilon_{f_D} T_I(2k+1) + 2\varepsilon_{\phi_0}}{2}\right) cos\left(\frac{2\pi\varepsilon_{f_D} T_I}{2}\right) \\ sin\left(2\pi\varepsilon_{f_D} t_0 + \varepsilon_{\phi_0}\right) \end{array} \right) \\
= & \frac{1}{\pi\varepsilon_{f_D} T_I}\left(\begin{array}{c} -sin\left(\pi\varepsilon_{f_D} T_I(2k+1) + \varepsilon_{\phi_0}\right) cos\left(\pi\varepsilon_{f_D} T_I\right) \\ +sin\left(2\pi\varepsilon_{f_D} t_0 + \varepsilon_{\phi_0}\right) \end{array} \right) \\
= & -sin\left(\pi\varepsilon_{f_D} T_I(2k+1) + \varepsilon_{\phi_0}\right) \frac{cos\left(\pi\varepsilon_{f_D} T_I\right)}{\pi\varepsilon_{f_D} T_I} + \frac{sin\left(2\pi\varepsilon_{f_D} t_0 + \varepsilon_{\phi_0}\right)}{\pi\varepsilon_{f_D} T_I}
\end{aligned}
$$